Supporting Information

Amine-Substituent Induced Highly Selective and Rapid "Turn-on" Detection of Carcinogenic 1,4-Dioxane from Purely Aqueous and Vapour phase with Novel Post-Synthetically Modified d^{10}-MOFs

Udayan Mondal,[a,b] Sourav Bej,[a.b] Abhijit Hazra,[a,b] Sukdeb Mandal,[a,b] Tapan K. Pal,[c] and Priyabrata Banerjee[a,b*]

[a] Surface Engineering & Tribology Group, CSIR-Central Mechanical Engineering Research Institute, Mahatma Gandhi Avenue, Durgapur 713209, West Bengal, India. E-mail addresses: pr_banerjee@cmeri.res.in, Webpage: www.cmeri.res.in and www.priyabratabanerjee.in.

[b] Academy of Scientific and Innovative Research (AcSIR), AcSIR Headquarters CSIR-HRDC Campus, Postal Staff College Area, Sector 19, Kamla Nehru Nagar, Ghaziabad-201002, Uttar Pradesh, India.

[c] Department of Chemistry, School of Technology, Pandit Deendayal Petroleum University, Gandhinagar-382007, India

Contents

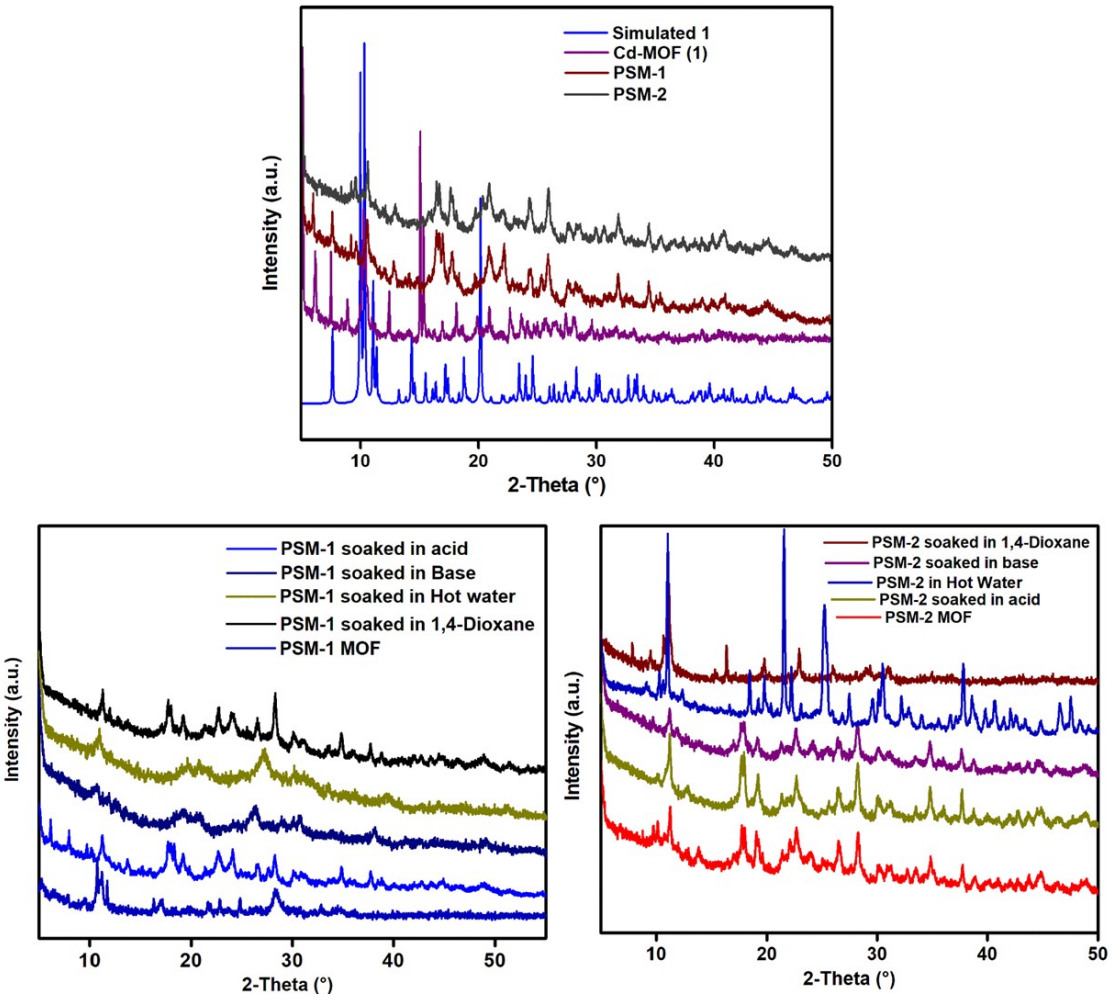

Fig S1. PXRD studies of (a) pristine Cd-MOF (both experimental and simulated), PSM-1 and PSM-2; (b) PSM-1 and (c) PSM-2 in distinct experimental conditions

SCXRD of 1

A suitable crystal of **1** with dimensions 0.24 × 0.16 × 0.10 mm^3 was selected and mounted on BRUKER SMART APEX-II CCD diffractometer. The crystal was kept at a steady T = 293(2) K during data collection. Data were collected using /w-scans with MoK_α radiation. The diffraction pattern was indexed and the total number of runs and images was based on the strategy calculation from the program Bruker APEX2.[15] The maximum resolution that was achieved was Θ = 25.099° (0.84 Å). The structure was solved with the ShelXT 2014/5 solution program using iterative methods and by using Olex2 1.5-dev as the graphical interface.[15] The model was refined with ShelXL 2018/3 (Sheldrick, 2015) using full matrix least squares minimisation on F^2.[15] The unit cell was refined using Bruker SAINT on 999 reflections, 4% of the observed reflections. Data reduction, scaling and absorption corrections were performed using Bruker SAINT.[15] The final completeness is 99.00 % out to 25.099° in *Θ*.SADABS.[15] The absorption coefficient μ of this material is 1.531 mm^{-1} at this wavelength (λ = 0.71073Å) and the minimum and maximum transmissions are 0.628 and 0.745.

The structure was solved and the space group $P2_1/n$ (#14) determined by the ShelXT 2014/5 structure solution program using iterative methods and refined by full matrix least squares minimisation on F^2 using version 2018/3 of ShelXL 2018/3.[15] All non-hydrogen atoms were refined anisotropically. Hydrogen atom positions were calculated geometrically and refined using the riding model.

Table S1: Crystallographic data of **1**

Parameters	Parent MOF (**1**)
Formula	$C_{36}H_{46}Cd_3N_7O_{16}$
Size (mm^3)	0.24 × 0.16 × 0.10 mm^3
Formula weight	1170.00
Temperature (K)	293(2)
Crystal system	Monoclinic
Space group	$P2_1/n$
a (Å)	13.3983(4)
b (Å)	10.3191(3)
c (Å)	16.2707(5)
α (°)	90
β (°)	104.9880(10)
γ (°)	90
Volume ($Å^3$)	2173.03(11)
Z	2
Z’	0.5
Wavelength/Å	0.71073
Radiation type	MoK_α
Θ_{min}/°	2.645
Θ_{max}/°	25.099
$D_{calc.}$ ($g.cm^{-3}$)	1.773
μ (mm^{-1})	1.531
F (000)	1160.0
S	1.093
h, k, l max	15,12,19
N_{ref}	3827
Tmin, Tmax	0.628,0.745
Measured Refl's.	22224
Indep't Refl's.	3827
Refl's I≥2 σ(I)	3366
R_{int}	0.0443
Parameters	387
Restrains	109
Largest peak	1.035
Deepest hole	-0.700
GooF	1.125
wR_2 (all data)	0.0926
wR_2	0.0828
R_1 (all data)	0.0430
R_1	0.0346

Table S2. Structure Quality Indicators:

Reflections:	d min (Mo) 2Θ= 50.2° 0.84	I/σ(I) 41.0	R_{int} 4.43%	Full 50.2° 99.1
Refinement:	Shift -0.001	Max Peak 1.0	Min Peak -0.7	GooF 1.125

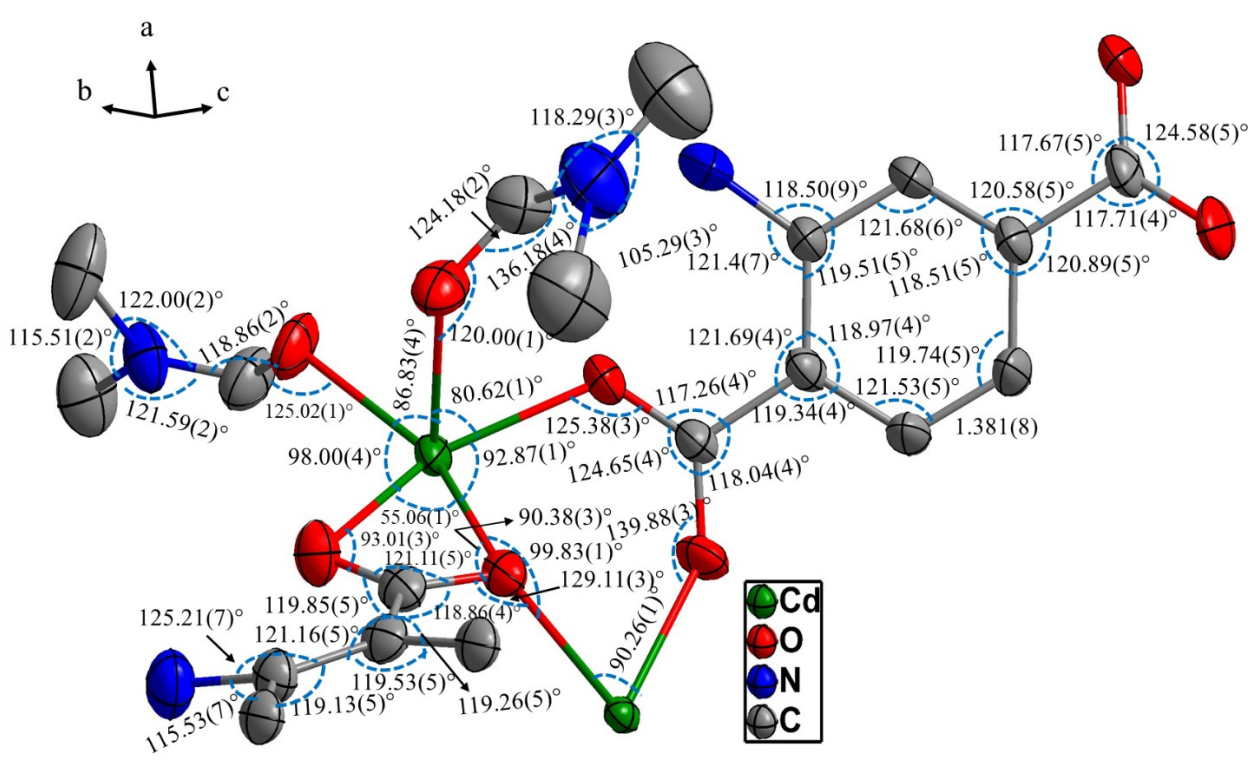

Fig. S2 Atomic anisotropic displacement parameters (ADPs) in terms of bond angle(°) for **1** [The perspective view of the asymmetric unit of 1 with 30% ellipsoid. The two disordered DMF molecules are removed for clarity of presentation]

Table S3. Selected Bond lengths in Å for **1**:

Atom	Atom	Length/Å
Cd1	O2	2.231(3)
Cd1	O2[1]	2.231(3)
Cd1	O4[2]	2.232(3)
Cd1	O4[3]	2.232(3)
Cd2	O5	2.357(4)
Cd2	O6	2.404(3)
Cd2	O8A	2.244(14)
Cd2	O8B	2.268(14)
Cd1	O6[1]	2.317(3)
Cd1	O6	2.317(3)
Cd2	O1	2.200(3)
Cd2	O3[3]	2.205(4)
Cd2	O9B	2.360(4)

[1]-x,-y,-z; [2]1/2-x,1/2+y,1/2-z;
[3]-1/2+x,-1/2-y,-1/2+z; [4]-x,1-y,-z

Table S4. Selected Bond Angles in ° for **1**:

Atom	Atom	Atom	Angle/°
O2	Cd1	O2[1]	180.0
O2[1]	Cd1	O4[2]	84.26(16)
O2[1]	Cd1	O4[3]	95.74(16)
O2	Cd1	O4[2]	95.74(16)
O2	Cd1	O4[3]	84.26(16)
O2	Cd1	O6[1]	89.76(13)
O2	Cd1	O6	90.24(13)
O2[1]	Cd1	O6[1]	90.24(13)
O2[1]	Cd1	O6	89.76(13)
O4[2]	Cd1	O4[3]	180.0(3)
O4[3]	Cd1	O6	91.04(15)
O4[3]	Cd1	O6[1]	88.96(15)
O4[2]	Cd1	O6[1]	91.04(15)
O4[2]	Cd1	O6	88.96(15)
O6[1]	Cd1	O6	180.0
O1	Cd2	O3[2]	101.99(17)
O1	Cd2	O5	146.17(15)
O1	Cd2	O6	92.87(13)
O1	Cd2	O8A	111.1(4)
O1	Cd2	O8B	91.7(4)
O1	Cd2	O9B	80.60(16)
O3[2]	Cd2	O5	99.11(16)
O3[2]	Cd2	O6	109.10(13)
O3[2]	Cd2	O8A	81.1(4)
O3[2]	Cd2	O8B	84.1(4)
O3[2]	Cd2	O9B	167.84(15)
O5	Cd2	O6	55.06(12)
O5	Cd2	O9B	84.31(16)
O8A	Cd2	O5	98.0(4)
O8A	Cd2	O6	151.8(4)
O8A	Cd2	O9B	86.8(4)
O8B	Cd2	O5	116.6(4)
O8B	Cd2	O6	164.7(5)
O8B	Cd2	O9B	83.9(4)
O9B	Cd2	O6	82.48(13)

[1]-x,-y,-z; [2]-1/2+x,-1/2-y,-1/2+z; [3]1/2-x,1/2+y,1/2-z; [4]1/2+x,-1/2-y,1/2+z; [5]1/2-x,-1/2+y,1/2-z; [6]-x,1-y,-z

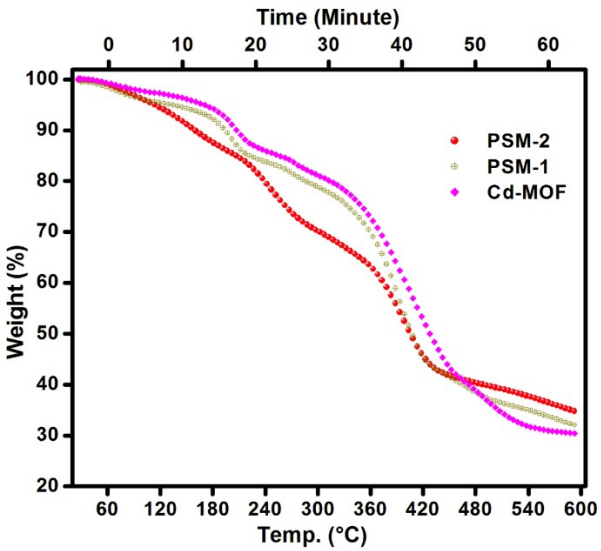

Figure S3. TGA curve of **Cd-MOF** (**1**), **PSM-1** and **PSM-2** under a nitrogen atmosphere

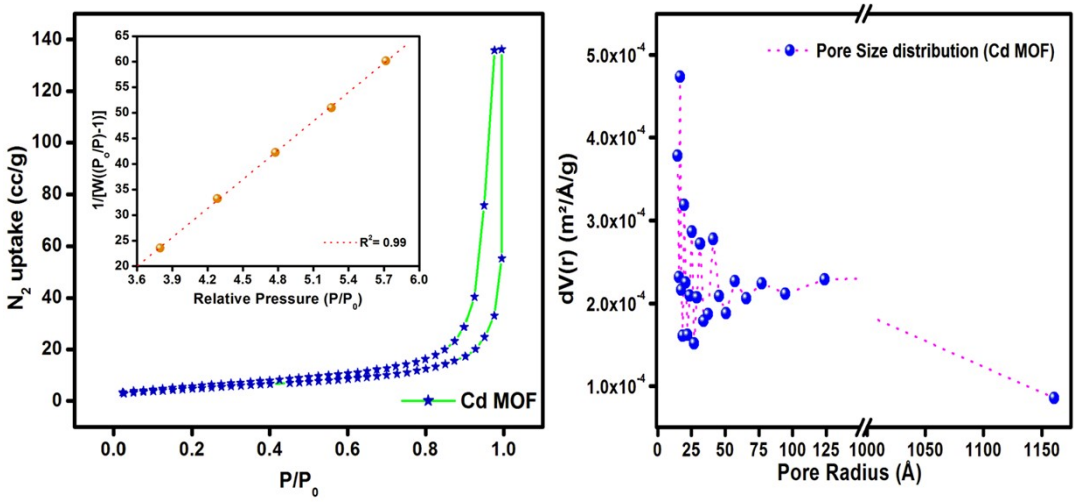

Fig. S4 surface area analysis of Cd-MOF (**1**)

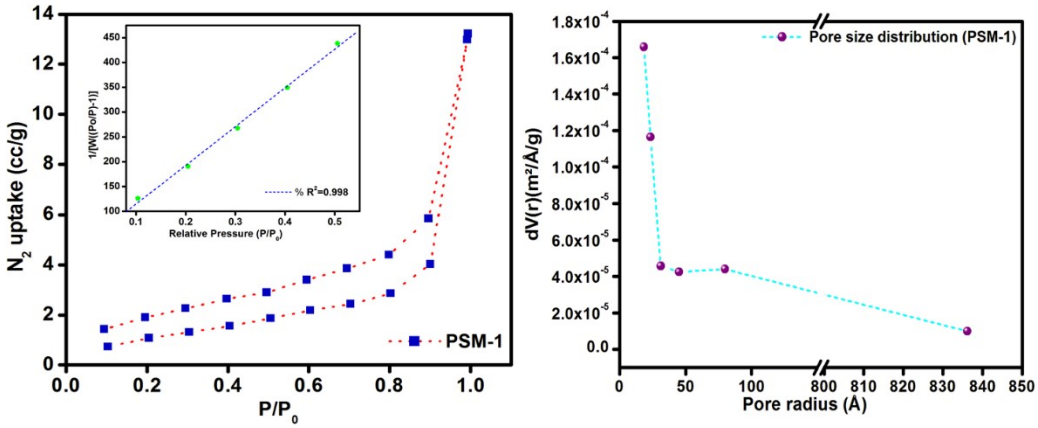

Fig. S5 surface area analysis of **PSM-1**

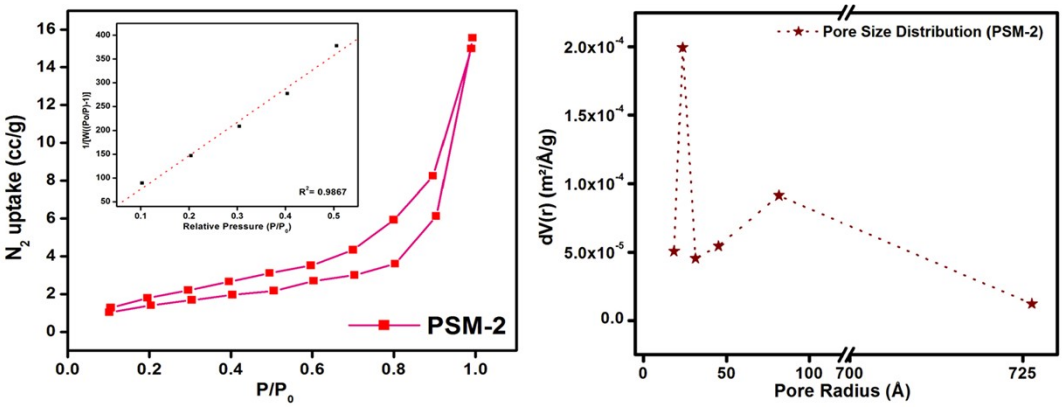

Fig. S6 surface area analysis of **PSM-2**

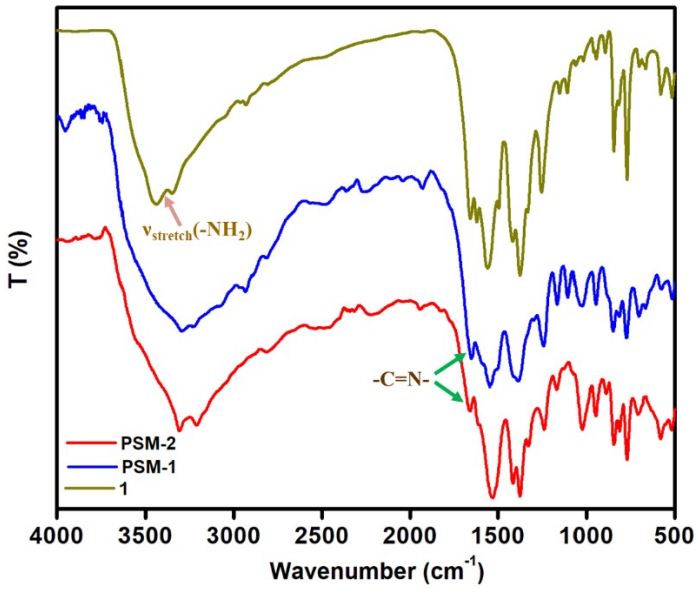

Fig. S7 FT-IR spectra of Cd-MOF (**1**), **PSM-1** and **PSM-2**

Acid Digestion Protocol: Briefly, ~20 mg of **PSM-1** and **PSM-2** were separately digested in 2-3.5 mL of methanol (HPLC grade) by the treatment with 300 µL of 35% of highly corrosive hydrofluoric acid (HF). Next, a slight amount of sodium bicarbonate ($NaHCO_3$) was added to this until neutral pH was attained. $NaHCO_3$ was added to avoid putting the imine (C=N) bonds in highly acidic atmosphere (imine hydrolysis can occur ultimately breaking C=N moiety). After around 30 minutes, the reaction mixtures were filtered diluted with adding HPLC grade methanol for further studies.

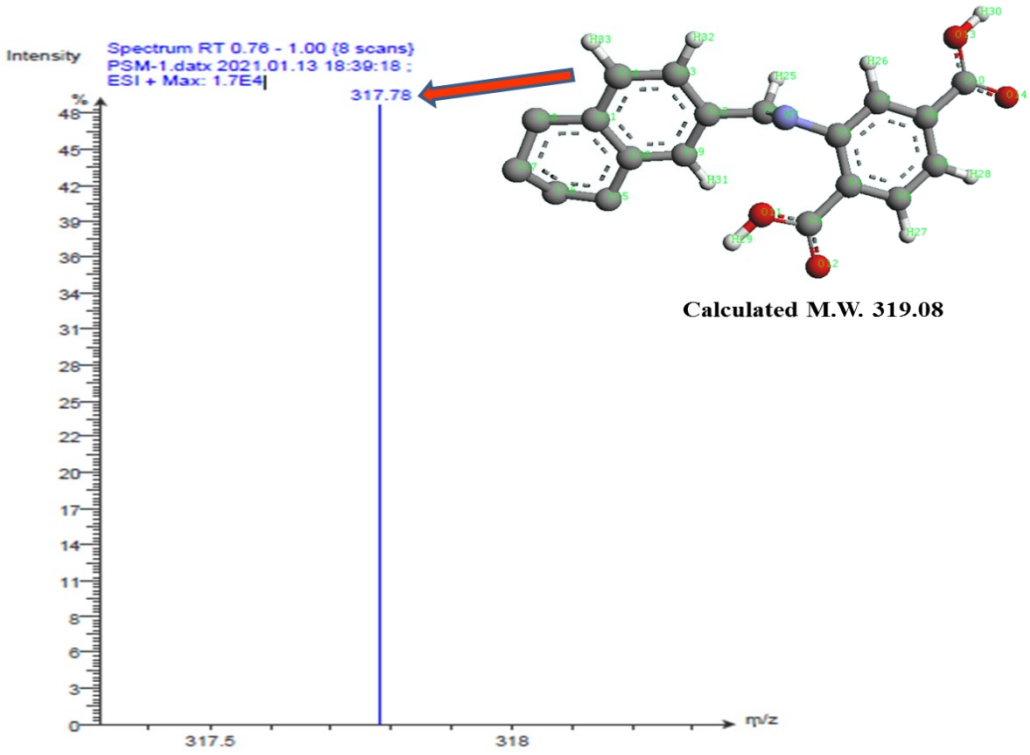

Fig. S8. ESI-MS spectra of the digested **PSM-1** fragment

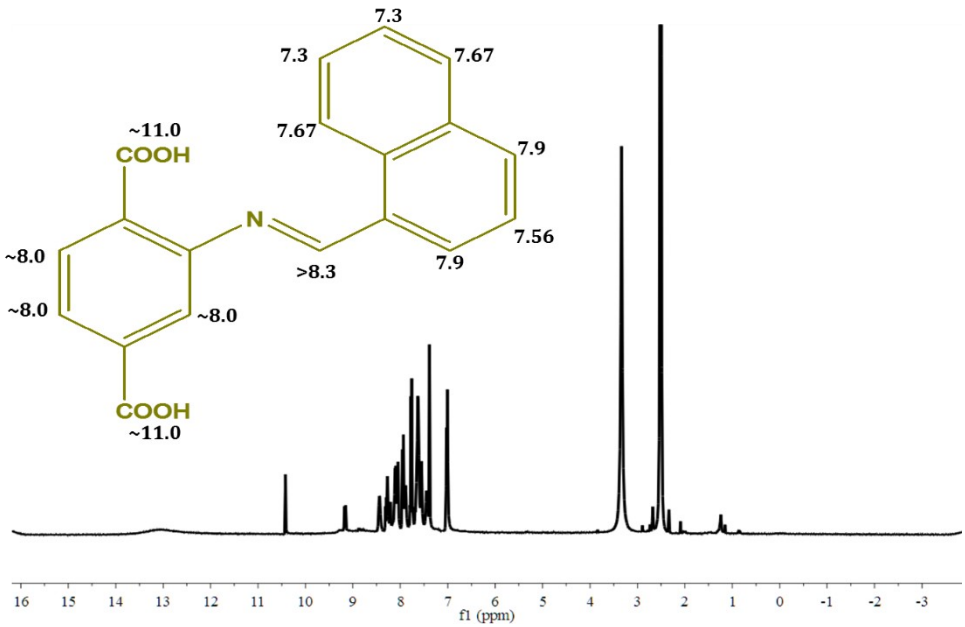

Fig. S9 ^{1}H-NMR of the digested **PSM-1** fragment

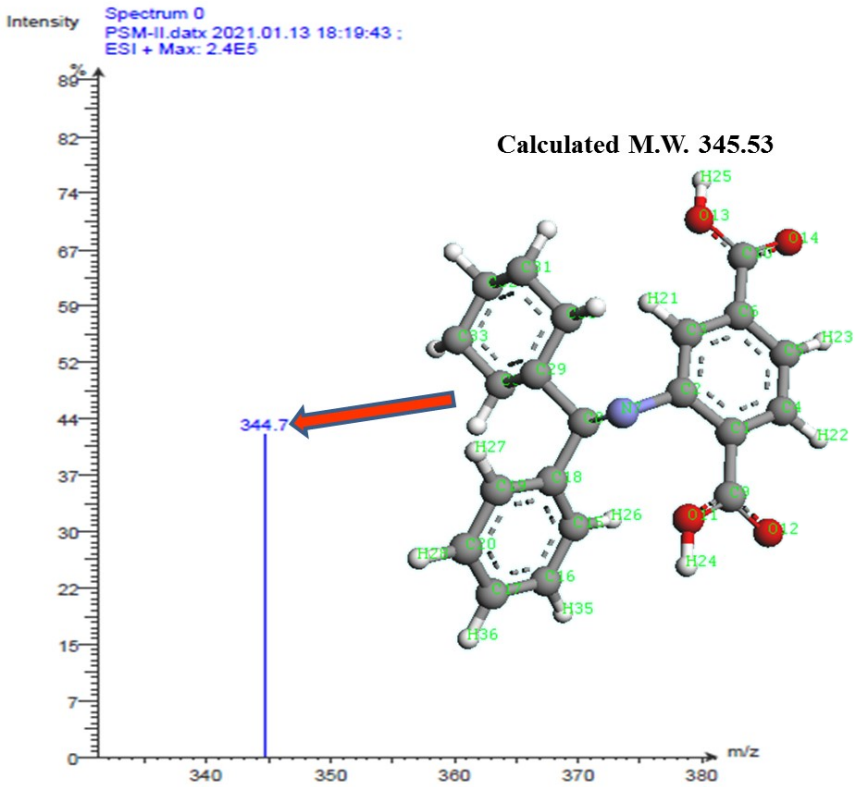

Fig. S10. ESI-MS spectra of acid-digested **PSM-2** fragment

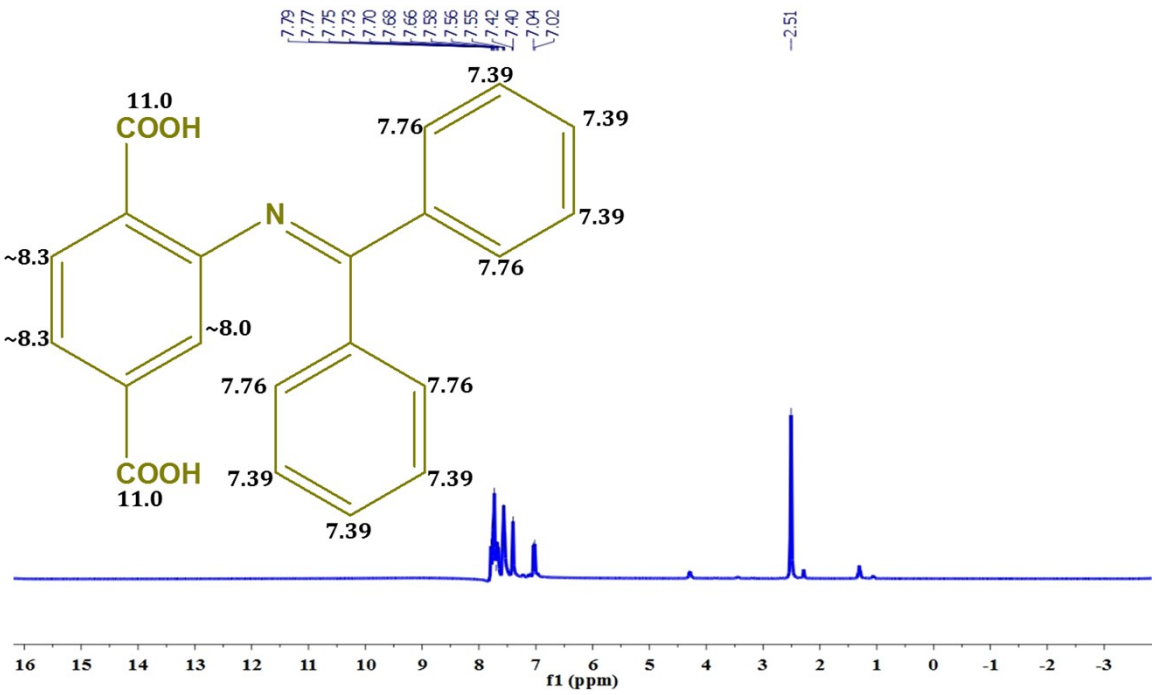

Fig. S11 ^{1}H-NMR of acid-digested **PSM-2** fragment

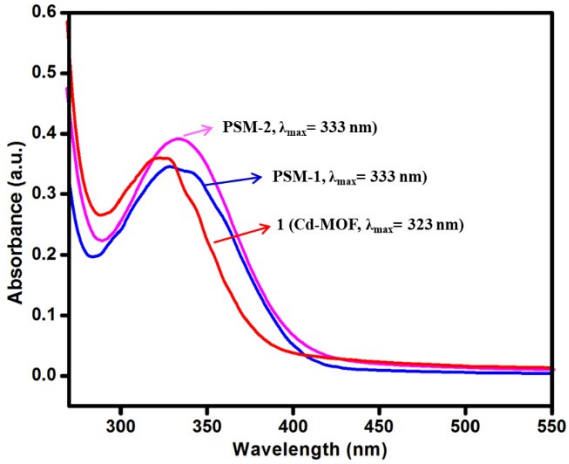

Fig. S12. Absorption spectra of **1, PSM-1** and **PSM-2**

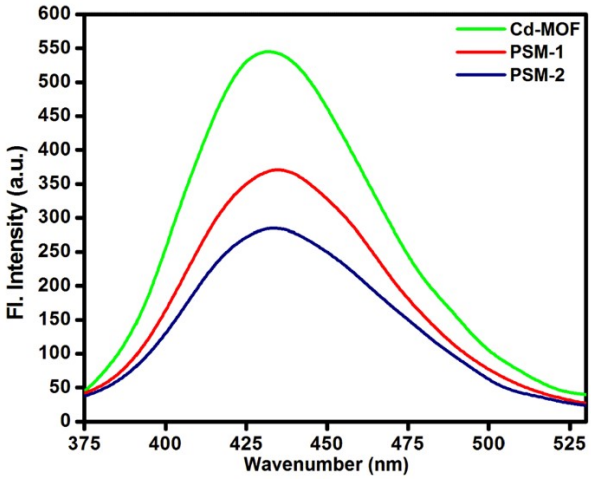

Fig. S13. Emission spectra of **Cd-MOF** (**1**), **PSM-1** and **PSM-2**

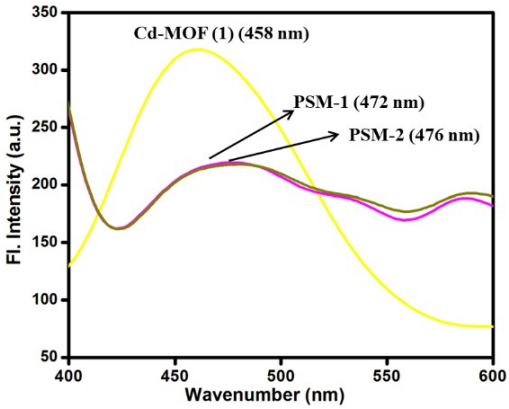

Fig. S14. Solid state emission spectra of **1**, **PSM-1**, and **PSM-2**

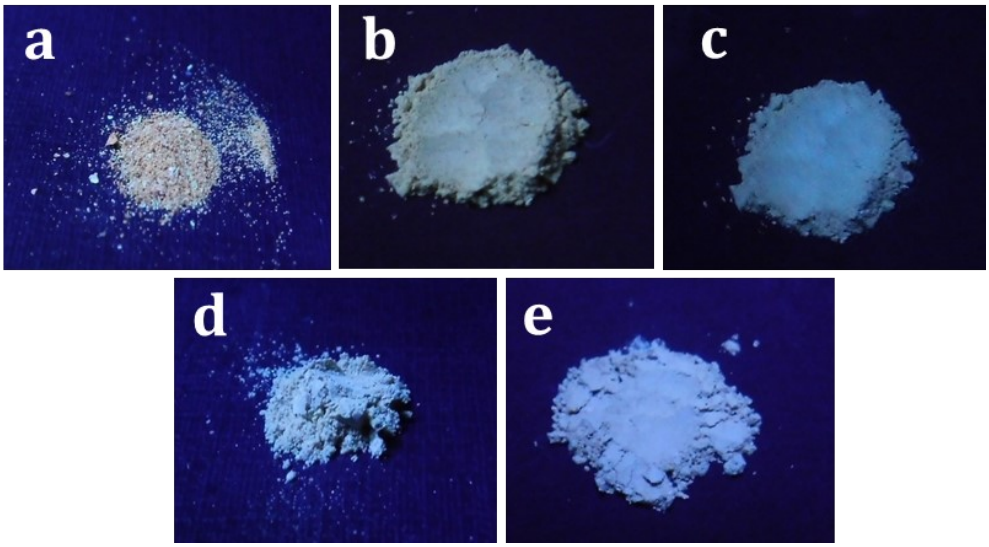

Fig. S15. Physical images of solid (a) **1**, (b) PSM-1, (c) PSM-2, (d) PSM-1+1,4-dioxane; (e) PSM-2+1,4-dioxane taken under handheld UV torch.

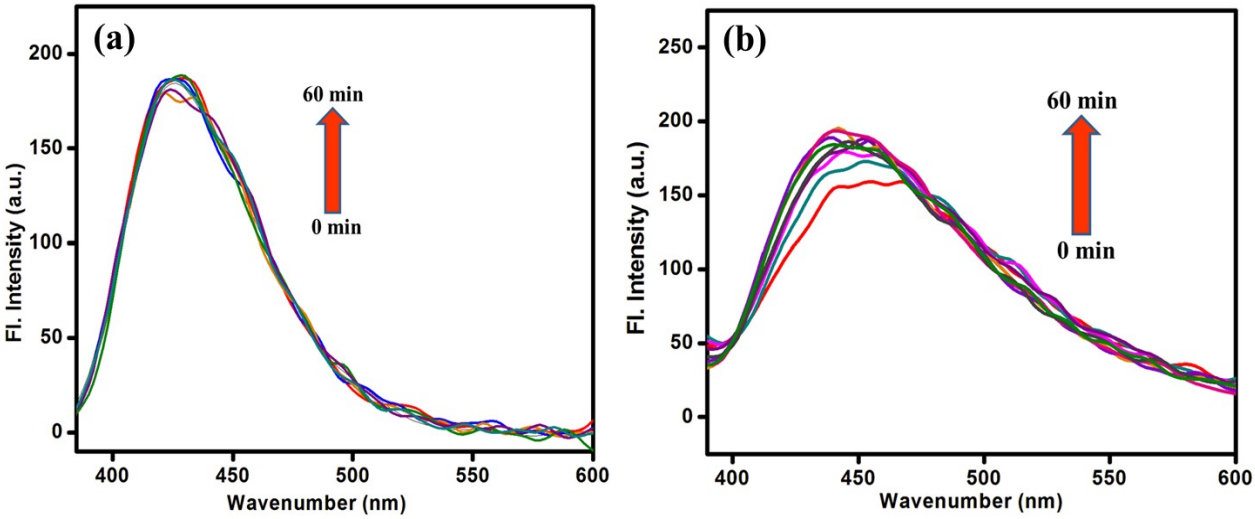

Fig. S16. Photostability of **PSM-1** and **PSM-2** (time: up to 60 minutes)

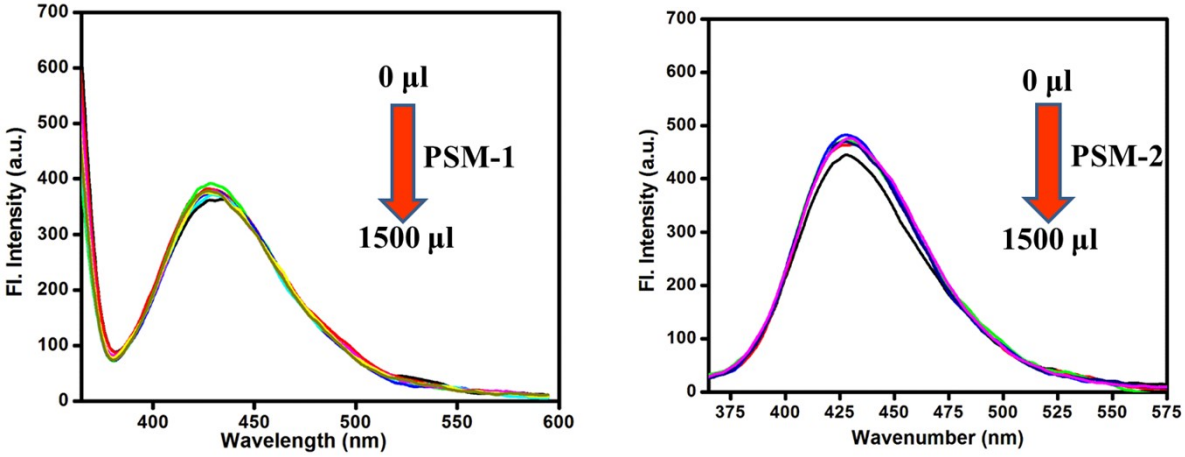

Fig. S17. Effect of addition of DI water to **PSM-1** and **PSM-2**

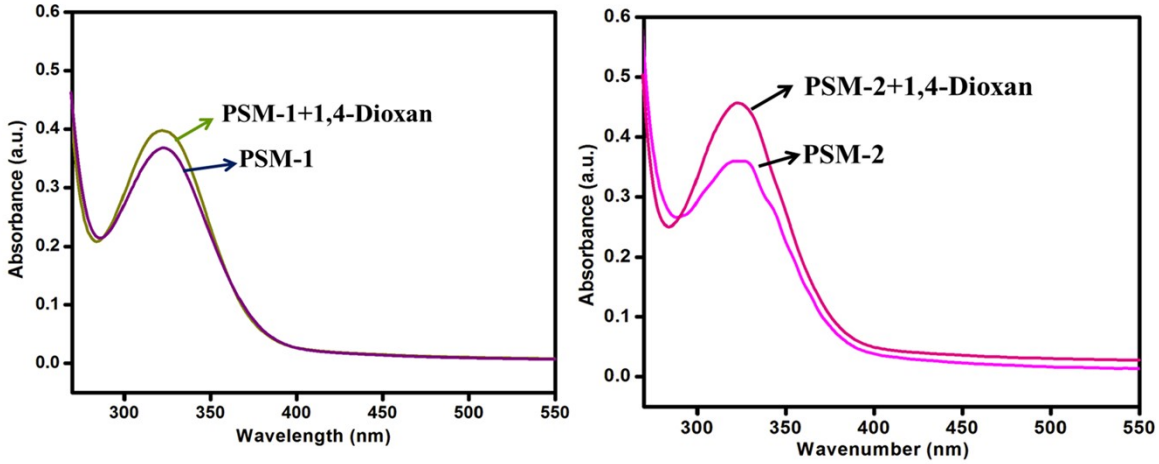

Fig. S18. Absorption spectra of **PSM-1** and **PSM-2** after 1,4-dioxan addition

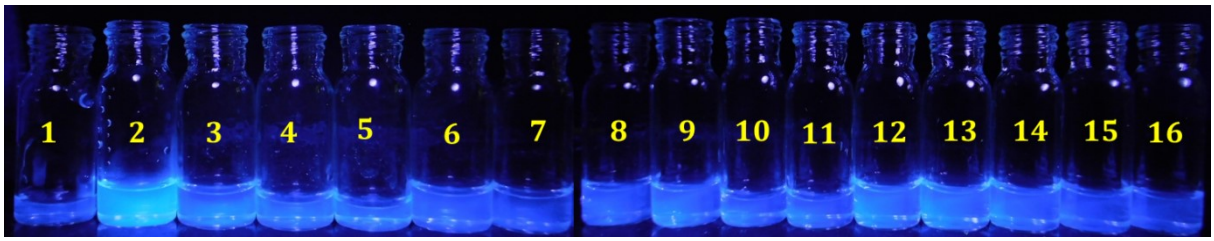

Fig. S19 Visual response of chemoreceptor **PSM-1** (1 mg dispersed in 5 ml DI water) towards various solvents (1 x 10^{-4} M) in the aqueous medium, under UV light: 1. PSM-1 (200 µl), 2. PSM-1+1,4-Dioxan, 3. PSM-1+1,2-dichlorobenzene, 4. PSM-1+Acetonitrile, 5. PSM-1+Benzaldehyde, 6. PSM-1+ Benzene, 7. PSM-1+ Chlorobenzene, 8. PSM-1+DMF, 9. PSM-1+DMSO, 10. PSM-1+Hexane, 11. PSM-1+MeOH, 12. PSM-1+Tolune, 13. PSM-1+Acetone, 14. PSM-1+Diethyl ether, 15. PSM-1+Ethanol, 16. PSM-1+THF

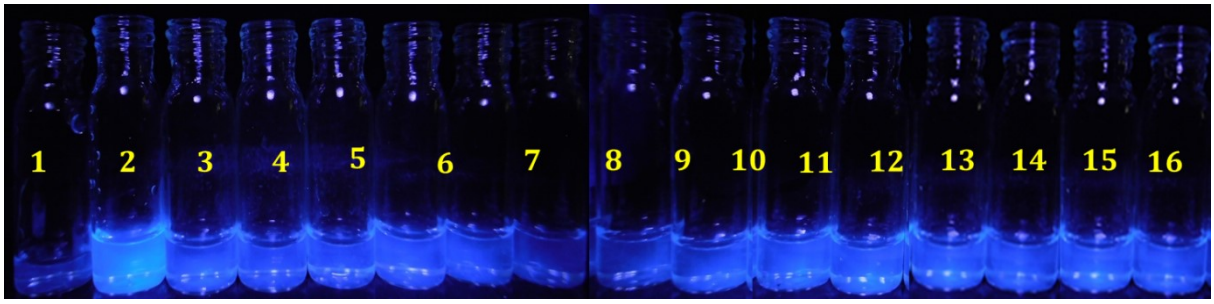

Fig. S20 Visual response of chemoreceptor **PSM-2** (1 mg dispersed in 5 ml distilled water) towards various solvents (1 x 10^{-4} M) in the aqueous medium, under UV light: 1. PSM-1 (200 µl), 2. PSM-1+1,4-Dioxan, 3. PSM-1+1,2-dichlorobenzene, 4. PSM-1+Acetonitrile, 5. PSM-1+Benzaldehyde, 6. PSM-1+ Benzene, 7. PSM-1+ Chlorobenzene, 8. PSM-1+DMF, 9. PSM-1+DMSO, 10. PSM-1+Hexane, 11. PSM-1+MeOH, 12. PSM-1+Tolune, 13. PSM-1+Acetone, 14. PSM-1+Diethyl ether, 15. PSM-1+Ethanol, 16. PSM-1+THF

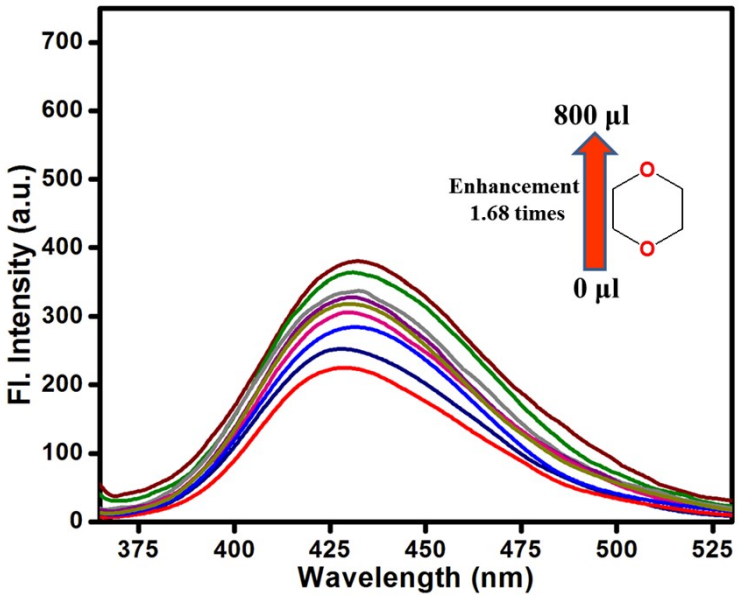

Figure S21. Fluorescence enhancement after gradual addition of 1,4-dioxane with **1**

The fluorescence titrations were carried out maintaining the PL conditions: excitation slit 10 nm, emission slit 10 nm, scan speed 800 nm/min.

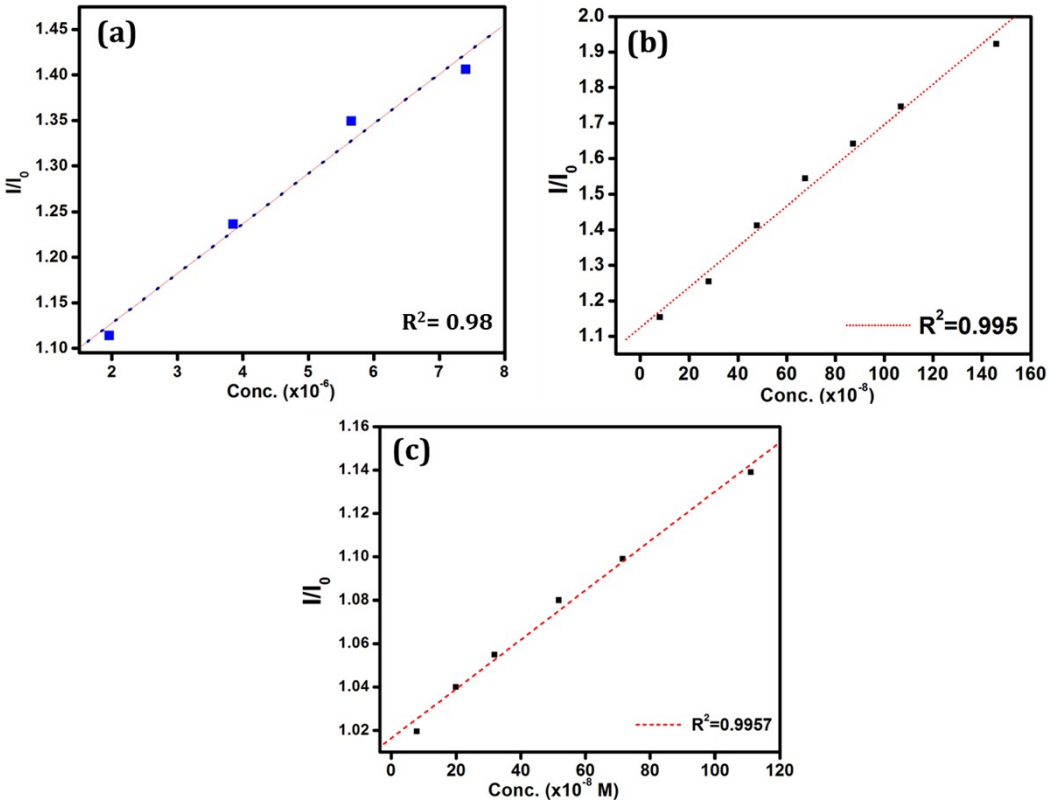

Figure S22. I/I_0 vs Conc. Plots of (a) **1**, (b) **PSM-1** and (c) **PSM-2**

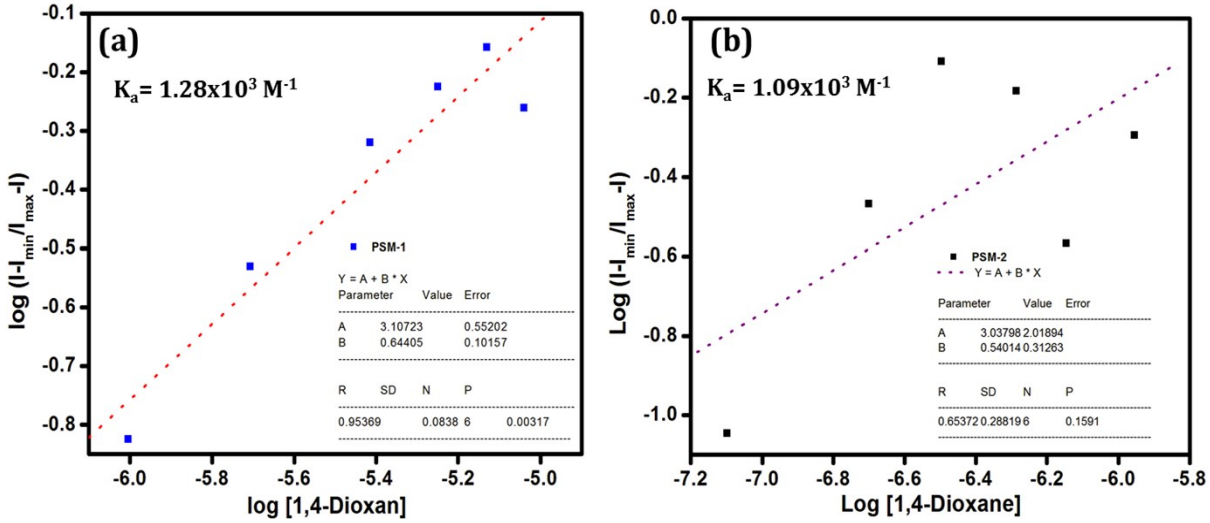

Figure S23. Plot of Log (I-I_{min}/I_{max}-I) vs. Log[1,4-dioxan] by Benesi–Hildebrand method for determination of association constant: (a) **PSM-1** and (b) **PSM-2**

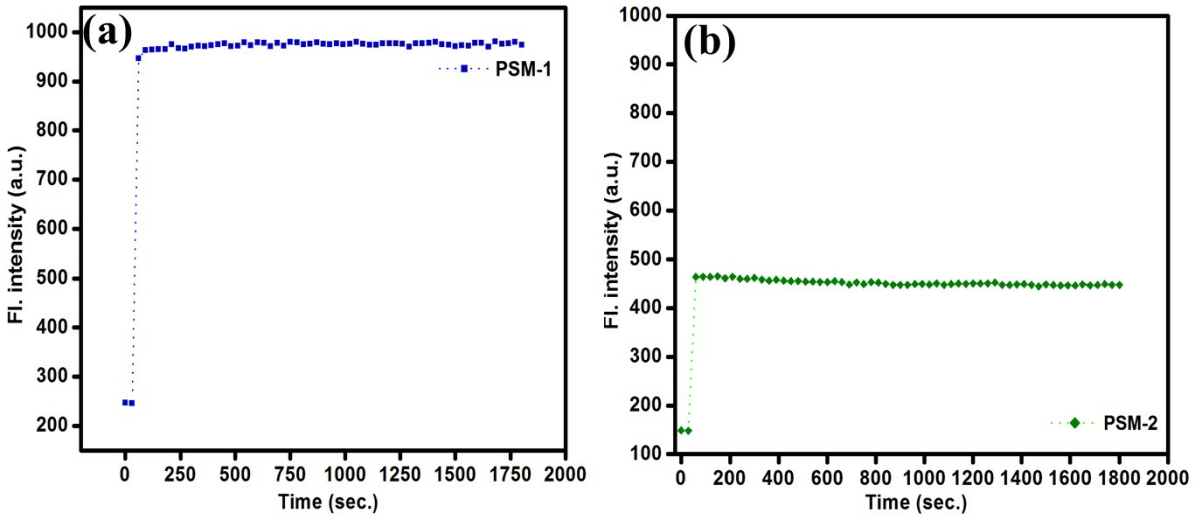

Fig. S24. Fluorescence enhancement based kinetic study: response time during 1,4-dioxane addition to **PSM-1** and **PSM-2**

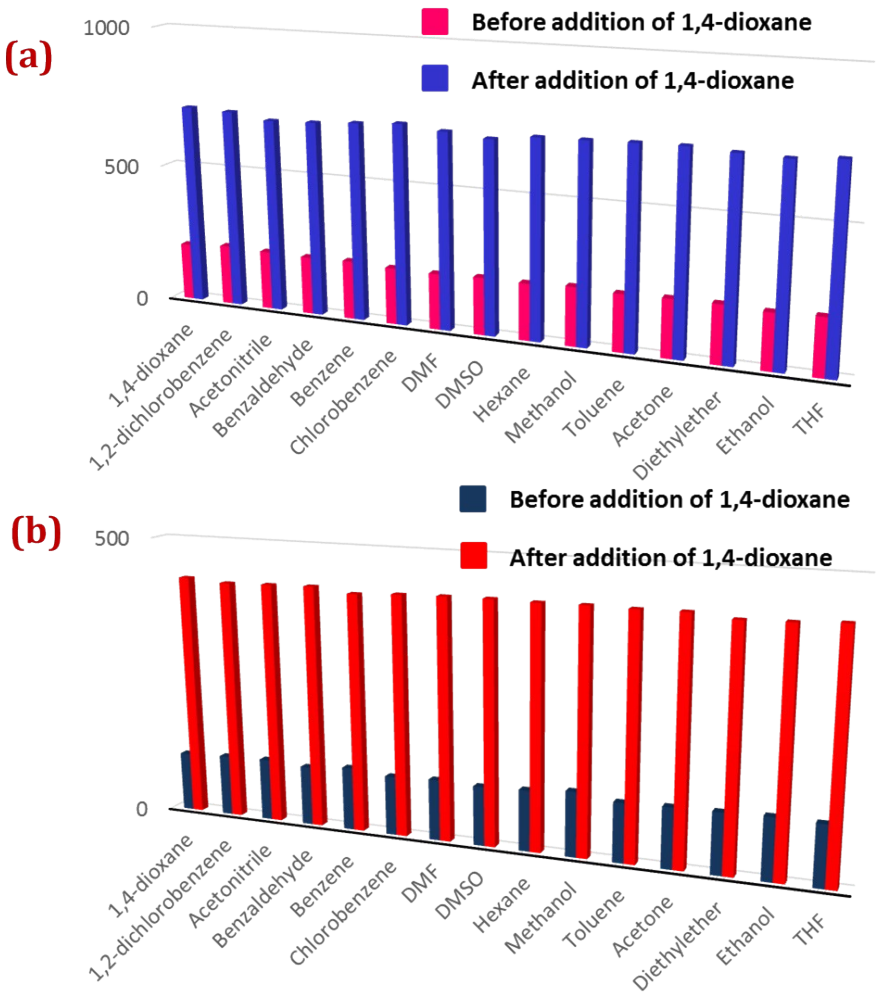

Fig. S25. Interference study of **PSM-1** and **PSM-2**

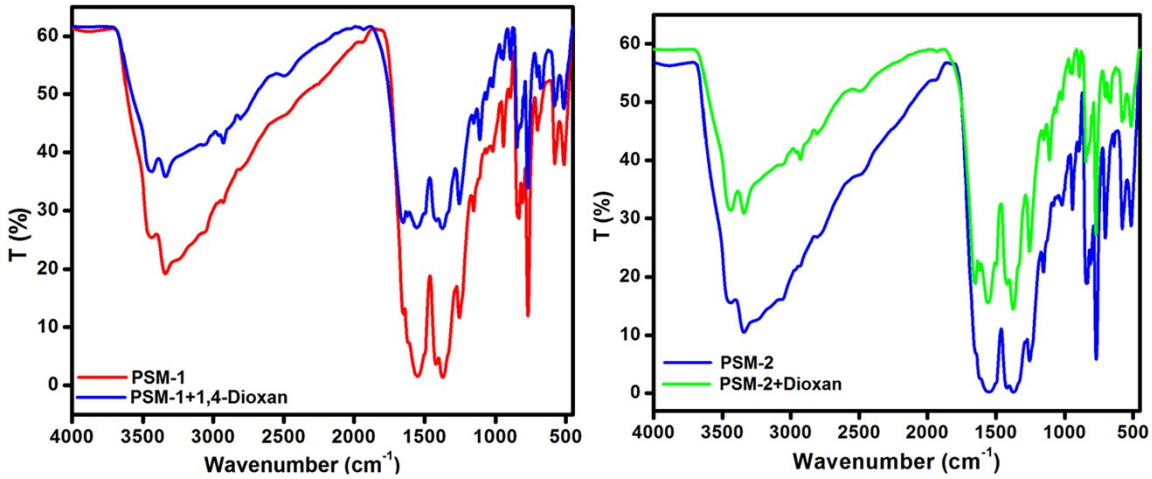

Fig. S26. FT-IR spectra of **PSM-1** and **PSM-2** after immersion in 1,4-dioxan (~6 h)

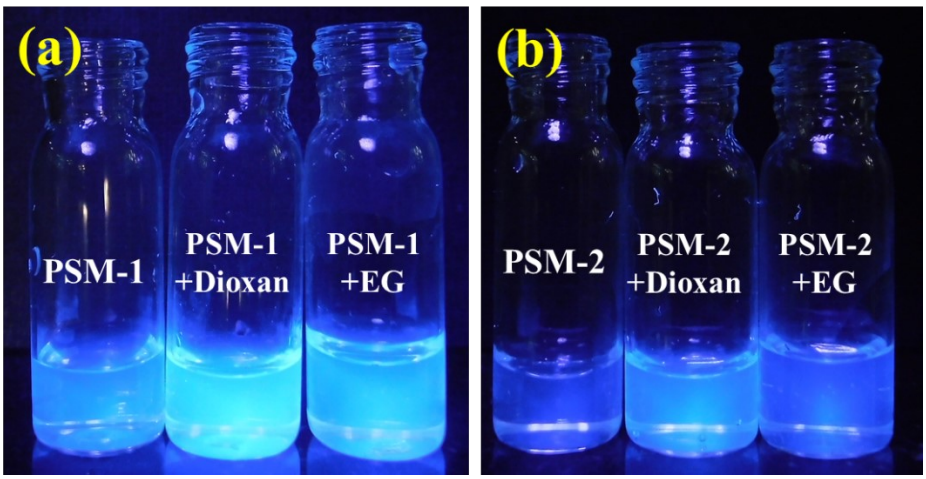

Fig. S27. Physical image during addition of EG to the sensor solutions: (a) **PSM-1** and (b) **PSM-2** (under UV irradiation)

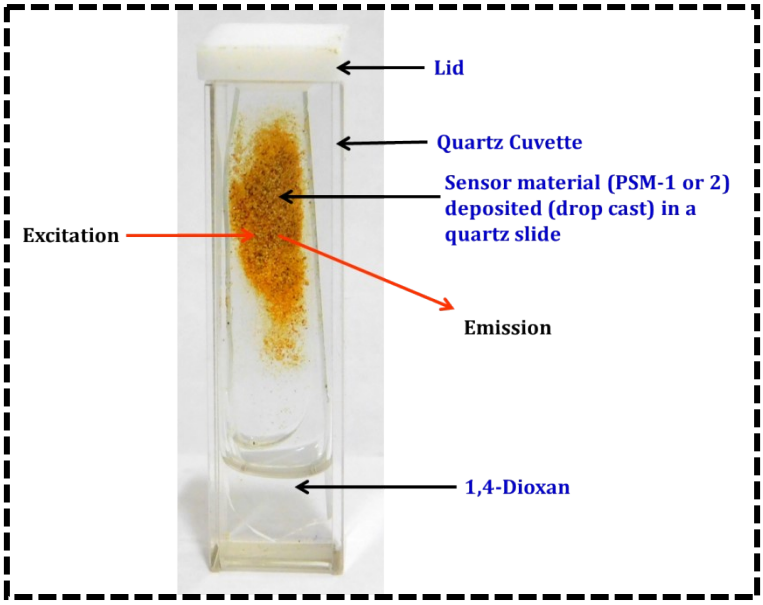

Fig. S28. Set-up for vapour phase sensing of 1,4-dioxan by developed sensor materials.

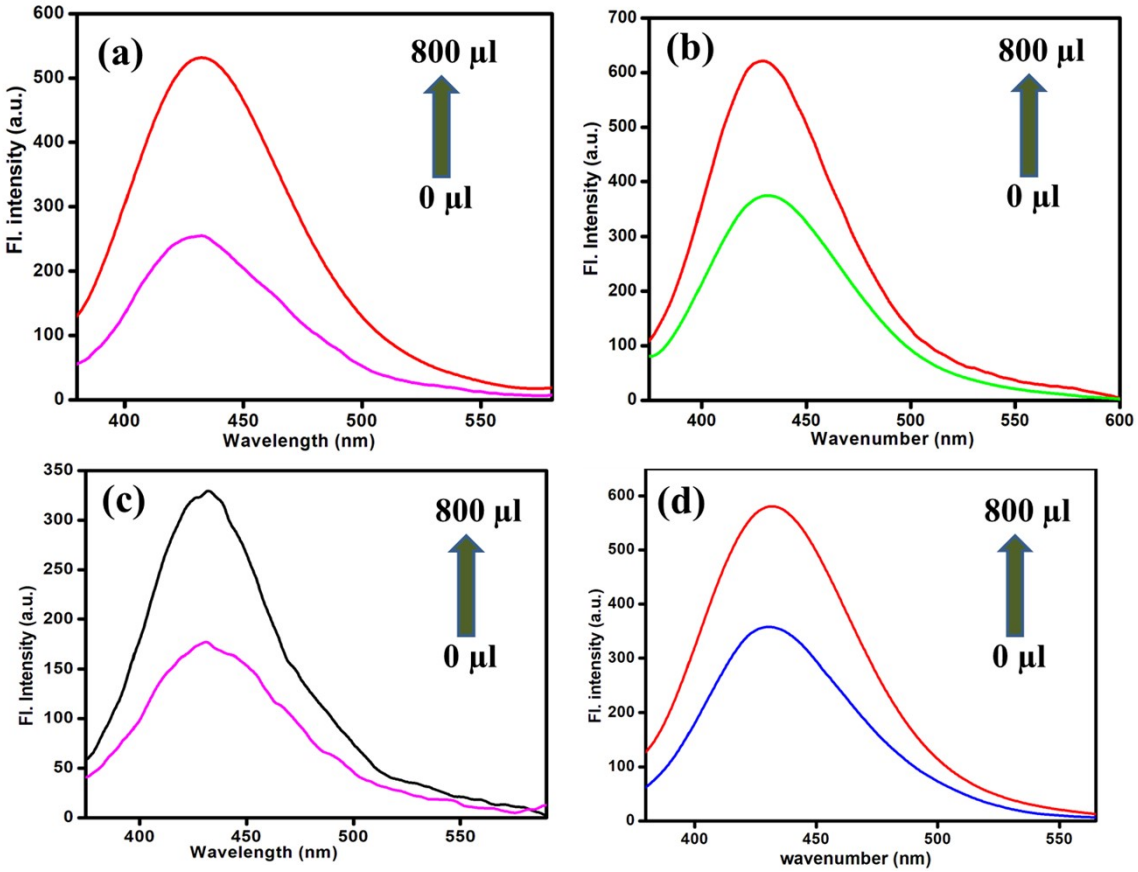

Fig. S29. Addition of 1,4-dioxane spiked real water samples to **PSM-1** (dispersed in DI water); (a) Effluent Treatment (ET) plant of CSIR-CMERI, (b) Damodar river water; (c) Canal water; (d) local sewage water

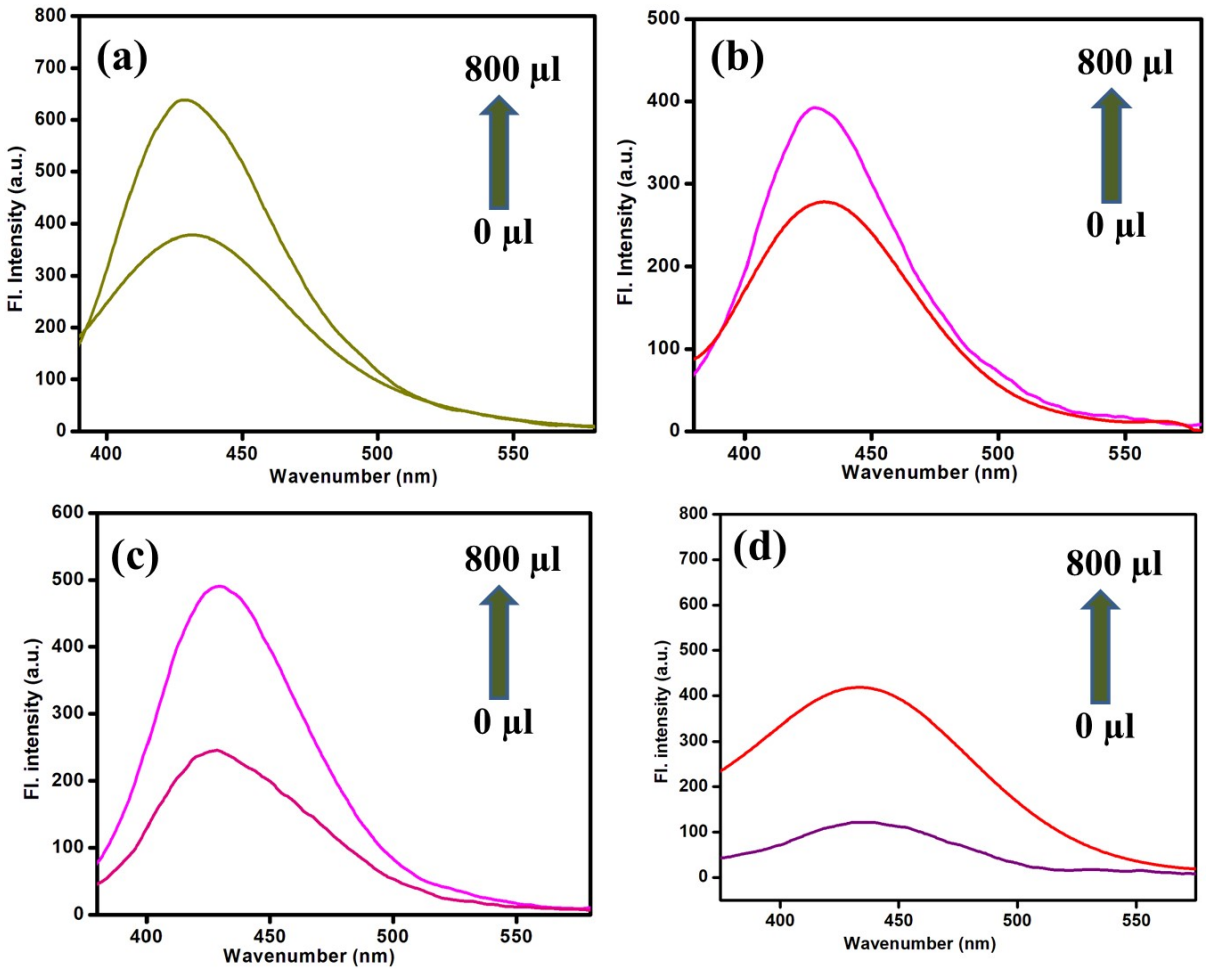

Fig. S30. Addition of 1,4-dioxan spiked real water samples to **PSM-2** (dispersed in DI water); (a) untreated water from Effluent Treatment Plant (ETP) of CSIR-CMERI, (b) Canal water; (c) local sewage water; (e) water of River Damodar, India.

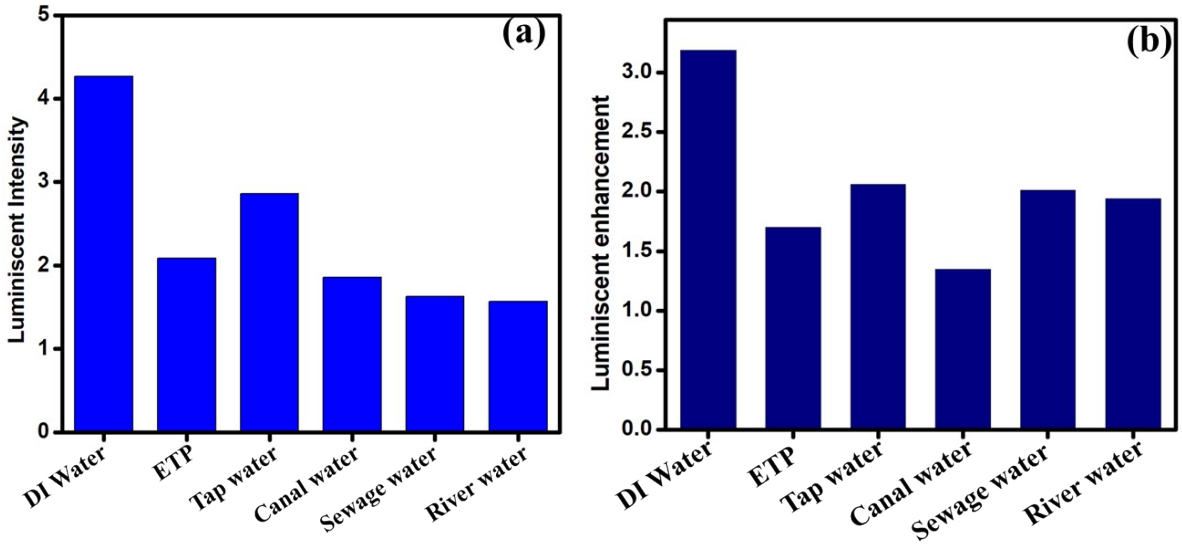

Fig. S31. Luminescence enhancement upon addition of 1,4-dioxane spiked real water samples collected from various parts of Durgapur industrial belt, India: (a) **PSM-1** and (b) **PSM-2**.

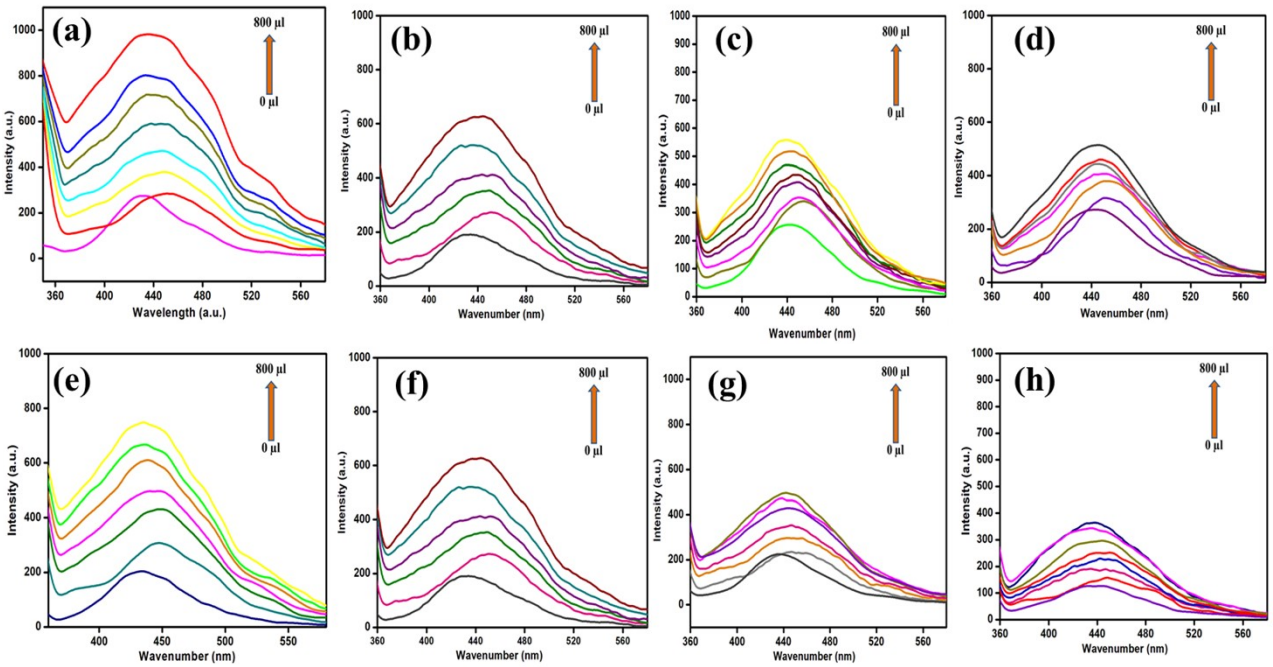

Fig. S32. Fluorescence emission enhancement during addition of 1,4-dioxane spiked cosmetic products extracted test portions: (a-d) **PSM-1:** (a) face wash (recovery: ~89.2%), (b) Body gel (recovery: ~73%), (c) cream (recovery: ~55%), (d) shampoo (recovery: ~52%); (e-h) **PSM-2:** (a) face wash (recovery: ~114%), (b) Body gel (recovery: ~96%), (c) cream (recovery: ~73%), (d) shampoo (recovery: ~95%).

Table S5. Comparative Literature Study regarding 1,4-Dioxane sensors

Entry	Sensor	Sensing medium	Sensing Method	Detection Limit	Vapour phase Sensing	Real field trial	Ref.
1.	Citrate stabilized silver nanoparticle (Ci-AgNP)	Water	Colorimetric	1 ppm	Yes	Yes	1
2.	NiO@Nd_2O_3 nanocomposites embedded on glassy carbon electrode	Water	Electrochemical	0.029 µA μM^{-1} cm^{-2}	No	Yes	2
3.	TB-TZ-COP (covalent organic polymer)	Ethylene glycol or direct addition	'Turn-on' fluorescent and colorimetric sensor	22.2 ppm	Yes	No	3
4.	Porous Organic Polymer: POP-HT	Direct addition in dioxan	Luminescence enhancement	--	No	No	4
5.	80-µm CAR–PDMS metal fibers	Water	SPME followed by either GC-FID or GC-MS	2.5 µg/L (ppb)	No	Yes	5
6.	--	Water	Frozen Micro-Extraction with GC/MS	1.6 µg/L	No	Yes	6
7.	Direct injection in GC-FID	Palm-based fatty alcohol ethoxylate	GC-FID	10-30 µg/g	No	No	7
8.	PAni-SiO_2 nanocomposites	Water	Electrochemical Sensing (deposited on GCE)	16.0 ± 0.8 pmol L^{-1}	No	Yes	8
9.	Combination of a mid-IR hollow waveguide with a FT-IR spectrometer, coupled with capillary membrane sampler.	--	Vapour phase detection by continuous liquid-gas extraction process	~15.6-123 ppm	No	Yes	9
10.	--	Aqueous medium	Heated Purge-and-Trap Preconcentration and	0.056-0.15 µg/L.	No	Yes	10

			GC-MS, with selected ion storage				
11.	--	Surfactants and cleaning agents	Headspace single-drop micro extraction with GC-FID	0.4 µg/g.	No	Aqueous cosmetic surfactant	11
12	Carbon nano-onion (CNO)	Aqueous Electrolyte	'Turn-on' fluorescent and electrochemical method	16.5 nM & 200 nM respectively	Yes	No	12
13	Activated carbon disks	Groundwater	Solid-phase extraction (SPE)	0.31 µg/L	No	Yes	13
14	GC–MS/MS instruments	Cosmetic ingredients	Pulsed split injection and electron ionization	0.2 µg/g	No	Real cosmetics	14
15.	**PSM-1 and PSM-2**	**Water medium**	**Fluorometric detection**	**12.25 µM & 28.33 µM respectively**	**Yes**	**Yes**	**Present work**

References:

1. A. Kumar, G. Vyas, M. Bhatt, S. Bhatt, P. Paul, ***Chem. Commun.***, 2015, 51, 15936-15939
2. Md. M. Rahman, A. Wahid and A. M. Asiri, ***New J. Chem.***, 2019, 43, 17395
3. S. Shanmugaraju, D. Umadevi, L. M. Gonzalez-Barcia, J. M. Delente, K. Byrne, W. Schmitt, G. W. Watson and T. Gunnlaugsson, ***Chem. Commun.***, 2019, 55, 12140
4. D. Ma, B. Li, Z. Cui, K. Liu, C. Chen, G. Li, J. Hua, B. Ma, Z. Shi, and S. Feng, ***ACS Appl. Mater. Interfaces***, 2016, 8, 24097−24103
5. R. E. Shirey and C. M. Linton, ***Journal of Chromatographic Science***, Vol. 44, August 2006.
6. M. Li, P. Conlon, S. Fiorenza, R. J. Vitale, and Pedro J.J. Alvarez, ***Ground Water Monitoring & Remediation 31***, no. 4/ Fall 2011/pages 70–76, DOI: 10.1111/j1745–6592.2011.01350.x
7. B. Y. P. Tay, Z. Maurad, H. Muhammad, ***J Am Oil Chem Soc.***, DOI: 10.1007/s11746-014-2471-9
8. M. R. Karima, M. M. Alam, M.O. Aijaz, A. M. Asiri, M.A. Dar, M. M. Rahman, ***Talanta*** 193 (2019) 64–69.
9. F. D. Meals, V. V. Pustogov, N. Croitoru and B. Mizaikoff, ***Applied Spectroscopy***, Volume 57, Number 6, 2003
10. M. Sun, C. Lopez-Velandia, and D. R. U. Knappe, ***Environ. Sci. Technol.***, 2016, 50, 5, 2246–2254.
11. M. Saraji and N. Shirvani, ***International Journal of Cosmetic Science***, 2017, 39, 36–41.
12. A. Panda, S. K. Arumugasamy, J. Lee, Y. Son, K. Yun, S. Venkateswarlu, M. Yoon, ***Applied Surface Science***, 537 (2021) 147872.
13. C. Issacson, T. K .G. Mohr., J. Field, ***Environ. Sci. Technol***. 2006, 40, 7305-7311.
14. W. Zhou, ***Journal of Chromatography A,*** 2019 (1607) 460400.
15. (a) International Tables for X-Ray Crystallography; Kynoch Press: Birmingham, England, 1952; Vol. III; (b) SAINT+, 6.02 ed.; Bruker AXS, Madison, WI, 1999; (c) G. M. Sheldrick, SADABS, Empirical Absorption Correction Program; University of Göttingen: Germany, 1997; (d) XPREP, 5.1 ed.; Siemens Industrial Automation Inc.: Madison, WI, 1995; (e) G. M. Sheldrick, SHELXL-2014, Program for Crystal Structure Refinement, University of Gottingen, Gottingen, Germany, 2018; (f) G. M. Sheldrick, SHELXTL Reference Manual, version 5.1, Bruker AXS, Madison, WI, 1997; (g) Spek, A. L.; Single-crystal structure validation with the program PLATON. J. Appl. Crystallogr. 2003, 36, 7-13; (h) APEX2 suite for crystallographic software, Bruker axs, Madison, WI; (i) O.V. Dolomanov and L.J. Bourhis and R.J. Gildea and J.A.K. Howard and H. Puschmann, Olex2: A complete structure solution, refinement and analysis program, *J. Appl. Cryst.*, (2009), **42**, 339-341; (j) SADABS, Bruker axs, Madison, WI; (k) G.M. Sheldrick, Crystal structure refinement with ShelXL, *Acta Cryst.*, (2015), **C71**, 3-8; (l) G. M. Sheldrick, ShelXT-Integrated space-group and crystal-structure determination, *Acta Cryst.*, (2015), **A71**, 3-8.